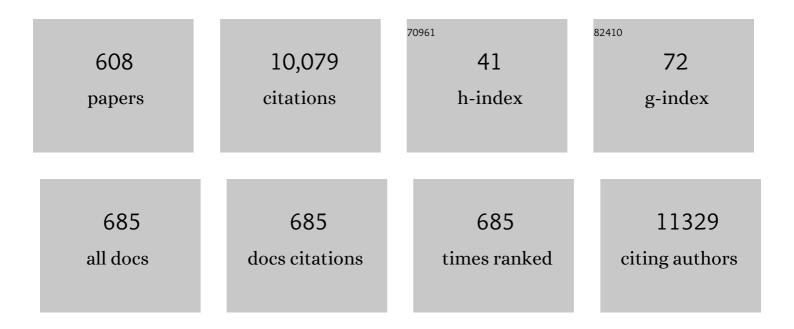
Andreas K Maier

List of Publications by Year in descending order

Source: https://exaly.com/author-pdf/6965134/publications.pdf Version: 2024-02-01



#	Article	IF	CITATIONS
1	The DELLA Domain of GA INSENSITIVE Mediates the Interaction with the GA INSENSITIVE DWARF1A Gibberellin Receptor of Arabidopsis. Plant Cell, 2007, 19, 1209-1220.	3.1	398
2	A gentle introduction to deep learning in medical image processing. Zeitschrift Fur Medizinische Physik, 2019, 29, 86-101.	0.6	344
3	Automatic classification of defective photovoltaic module cells in electroluminescence images. Solar Energy, 2019, 185, 455-468.	2.9	250
4	PEAKS – A system for the automatic evaluation of voice and speech disorders. Speech Communication, 2009, 51, 425-437.	1.6	214
5	Multi-Scale Deep Reinforcement Learning for Real-Time 3D-Landmark Detection in CT Scans. IEEE Transactions on Pattern Analysis and Machine Intelligence, 2019, 41, 176-189.	9.7	209
6	Automatic Classification of Cancerous Tissue in Laserendomicroscopy Images of the Oral Cavity using Deep Learning. Scientific Reports, 2017, 7, 11979.	1.6	194
7	Deep Learning Computed Tomography: Learning Projection-Domain Weights From Image Domain in Limited Angle Problems. IEEE Transactions on Medical Imaging, 2018, 37, 1454-1463.	5.4	166
8	Nucleophilic Reactivities of Primary and Secondary Amines in Acetonitrile. European Journal of Organic Chemistry, 2009, 2009, 6379-6385.	1.2	153
9	A global benchmark of algorithms for segmenting the left atrium from late gadolinium-enhanced cardiac magnetic resonance imaging. Medical Image Analysis, 2021, 67, 101832.	7.0	150
10	Kill-painting of hypoxic tumours in charged particle therapy. Scientific Reports, 2015, 5, 17016.	1.6	124
11	TOWARD QUANTITATIVE OPTICAL COHERENCE TOMOGRAPHY ANGIOGRAPHY. Retina, 2016, 36, S118-S126.	1.0	114
12	Robust Non-rigid Registration Through Agent-Based Action Learning. Lecture Notes in Computer Science, 2017, , 344-352.	1.0	112
13	Learning with known operators reduces maximum error bounds. Nature Machine Intelligence, 2019, 1, 373-380.	8.3	111
14	CONRAD—A software framework for coneâ€beam imaging in radiology. Medical Physics, 2013, 40, 111914.	1.6	106
15	Towards More Reality in the Recognition of Emotional Speech. , 2007, , .		89
16	Helium ions for radiotherapy? Physical and biological verifications of a novel treatment modality. Medical Physics, 2016, 43, 1995-2004.	1.6	87
17	Writer Identification Using GMM Supervectors and Exemplar-SVMs. Pattern Recognition, 2017, 63, 258-267.	5.1	85
18	Robust Multiframe Super-Resolution Employing Iteratively Re-Weighted Minimization. IEEE Transactions on Computational Imaging, 2016, 2, 42-58.	2.6	81

#	Article	IF	CITATIONS
19	Some Investigations on Robustness of Deep Learning in Limited Angle Tomography. Lecture Notes in Computer Science, 2018, , 145-153.	1.0	80
20	Classification of Breast Cancer Histology Images Using Transfer Learning. Lecture Notes in Computer Science, 2018, , 812-819.	1.0	78
21	The impact of model assumptions on results of computational mechanics in abdominal aortic aneurysm. Journal of Vascular Surgery, 2010, 51, 679-688.	0.6	73
22	Including oxygen enhancement ratio in ion beam treatment planning: model implementation and experimental verification. Physics in Medicine and Biology, 2013, 58, 3871-3895.	1.6	73
23	A Comparative Error Analysis of Current Time-of-Flight Sensors. IEEE Transactions on Computational Imaging, 2016, 2, 27-41.	2.6	71
24	Noise reduction in optical coherence tomography images using a deep neural network with perceptually-sensitive loss function. Biomedical Optics Express, 2020, 11, 817.	1.5	71
25	Evaluation of speech intelligibility for children with cleft lip and palate by means of automatic speech recognition. International Journal of Pediatric Otorhinolaryngology, 2006, 70, 1741-1747.	0.4	70
26	Age and gender recognition for telephone applications based on GMM supervectors and support vector machines. Proceedings of the IEEE International Conference on Acoustics, Speech, and Signal Processing, 2008, , .	1.8	70
27	Optical Coherence Tomography Angiography Characteristics of Iris Melanocytic Tumors. Ophthalmology, 2017, 124, 197-204.	2.5	67
28	Unsupervised Feature Learning for Writer Identification and Writer Retrieval. , 2017, , .		66
29	Photoreceptor Layer Thickness Changes During Dark Adaptation Observed With Ultrahigh-Resolution Optical Coherence Tomography. , 2017, 58, 4632.		61
30	X-ray-transform Invariant Anatomical Landmark Detection for Pelvic Trauma Surgery. Lecture Notes in Computer Science, 2018, , 55-63.	1.0	61
31	Demographic estimates of hunter–gatherers during the Last Glacial Maximum in Europe against the background of palaeoenvironmental data. Quaternary International, 2016, 425, 49-61.	0.7	55
32	Intraoperative Imaging Modalities and Compensation for Brain Shift in Tumor Resection Surgery. International Journal of Biomedical Imaging, 2017, 2017, 1-18.	3.0	55
33	ORCA-SPOT: An Automatic Killer Whale Sound Detection Toolkit Using Deep Learning. Scientific Reports, 2019, 9, 10997.	1.6	55
34	Deep Learning Computed Tomography. Lecture Notes in Computer Science, 2016, , 432-440.	1.0	54
35	Automatic detection of articulation disorders in children with cleft lip and palate. Journal of the Acoustical Society of America, 2009, 126, 2589-2602.	0.5	53
36	Automatic Cell Detection in Bright-Field Microscope Images Using SIFT, Random Forests, and Hierarchical Clustering. IEEE Transactions on Medical Imaging, 2013, 32, 2274-2286.	5.4	53

#	Article	IF	CITATIONS
37	Markerâ€free motion correction in weightâ€bearing coneâ€beam CT of the knee joint. Medical Physics, 2016, 43, 1235-1248.	1.6	50
38	Modulation of the peripheral immune system after low-dose radon spa therapy: Detailed longitudinal immune monitoring of patients within the RAD-ON01 study. Autoimmunity, 2017, 50, 133-140.	1.2	50
39	Adversarial and Perceptual Refinement for Compressed Sensing MRI Reconstruction. Lecture Notes in Computer Science, 2018, , 232-240.	1.0	50
40	Influence of acute hypoxia and radiation quality on cell survival. Journal of Radiation Research, 2013, 54, i23-i30.	0.8	49
41	Epipolar Consistency in Transmission Imaging. IEEE Transactions on Medical Imaging, 2015, 34, 2205-2219.	5.4	48
42	Automatic detection and analysis of photovoltaic modules in aerial infrared imagery. , 2016, , .		47
43	Next-generation imaging of the skeletal system and its blood supply. Nature Reviews Rheumatology, 2019, 15, 533-549.	3.5	46
44	Deep Generalized Max Pooling. , 2019, , .		45
45	Dynamic Iterative Reconstruction for Interventional 4-D C-Arm CT Perfusion Imaging. IEEE Transactions on Medical Imaging, 2013, 32, 1336-1348.	5.4	43
46	The Definition, Rationale, and Effects of Thresholding in OCT Angiography. Ophthalmology Retina, 2017, 1, 435-447.	1.2	43
47	Radon Exposure—Therapeutic Effect and Cancer Risk. International Journal of Molecular Sciences, 2021, 22, 316.	1.8	43
48	Influence of chronic hypoxia and radiation quality on cell survival. Journal of Radiation Research, 2013, 54, i13-i22.	0.8	42
49	NLO QCD corrections to W + W \hat{a}° b b \hat{A}^{-} \$\$ {W}^{+}{W}^{-} boverline{b} \$\$ production with leptonic decays in the light of top quark mass and asymmetry measurements. Journal of High Energy Physics, 2014, 2014, 1.	1.6	42
50	Offline Writer Identification Using Convolutional Neural Network Activation Features. Lecture Notes in Computer Science, 2015, , 540-552.	1.0	42
51	Technical Note: PYROâ€NN: Python reconstruction operators in neural networks. Medical Physics, 2019, 46, 5110-5115.	1.6	42
52	Automated Calculation of Alberta Stroke Program Early CT Score. Stroke, 2019, 50, 3277-3279.	1.0	42
53	Evaluation of MRI to Ultrasound Registration Methods for Brain Shift Correction: The CuRIOUS2018 Challenge. IEEE Transactions on Medical Imaging, 2020, 39, 777-786.	5.4	42
54	Fiducial marker-based correction for involuntary motion in weight-bearing C-arm CT scanning of knees. II. Experiment. Medical Physics, 2014, 41, 061902.	1.6	41

#	Article	IF	CITATIONS
55	Reconstruction of top-quark mass effects in Higgs pair production and other gluon-fusion processes. Journal of High Energy Physics, 2018, 2018, 1.	1.6	40
56	Deep learning algorithms out-perform veterinary pathologists in detecting the mitotically most active tumor region. Scientific Reports, 2020, 10, 16447.	1.6	39
57	Segmentation of photovoltaic module cells in uncalibrated electroluminescence images. Machine Vision and Applications, 2021, 32, 1.	1.7	39
58	Automated Detection of Motion Artefacts in MR Imaging Using Decision Forests. Journal of Medical Engineering, 2017, 2017, 1-9.	1.1	38
59	Weakly Supervised Segmentation of Cracks on Solar Cells Using Normalized L _p Norm. , 2019, , .		38
60	Deep Learning-Based Quantification of Pulmonary Hemosiderophages in Cytology Slides. Scientific Reports, 2020, 10, 9795.	1.6	38
61	Populations headed south? The Gravettian from a palaeodemographic point of view. Antiquity, 2017, 91, 573-588.	0.5	37
62	SkinNet: A Deep Learning Framework for Skin Lesion Segmentation. , 2018, , .		36
63	Encoding CNN Activations for Writer Recognition. , 2018, , .		36
64	Deep learning-based detection of motion artifacts in probe-based confocal laser endomicroscopy images. International Journal of Computer Assisted Radiology and Surgery, 2019, 14, 31-42.	1.7	36
65	Enhanced Crack Segmentation (eCS): A Reference Algorithm for Segmenting Cracks in Multicrystalline Silicon Solar Cells. IEEE Journal of Photovoltaics, 2019, 9, 752-758.	1.5	36
66	Automatic dementia screening and scoring by applying deep learning on clock-drawing tests. Scientific Reports, 2020, 10, 20854.	1.6	36
67	Deep Learning for Magnetic Resonance Fingerprinting: A New Approach for Predicting Quantitative Parameter Values from Time Series. Studies in Health Technology and Informatics, 2017, 243, 202-206.	0.2	36
68	Automatic Quantification of Speech Intelligibility of Adults with Oral Squamous Cell Carcinoma. Folia Phoniatrica Et Logopaedica, 2008, 60, 151-156.	0.5	35
69	Comparative study of deep learning models for optical coherence tomography angiography. Biomedical Optics Express, 2020, 11, 1580.	1.5	35
70	Indefinite kernels in least squares support vector machines and principal component analysis. Applied and Computational Harmonic Analysis, 2017, 43, 162-172.	1.1	34
71	Deep learning acceleration of Total Lagrangian Explicit Dynamics for soft tissue mechanics. Computer Methods in Applied Mechanics and Engineering, 2020, 358, 112628.	3.4	34
72	Automatic speech recognition (ASR) and its use as a tool for assessment or therapy of voice, speech, and language disorders. Logopedics Phoniatrics Vocology, 2009, 34, 91-96.	0.5	33

#	Article	IF	CITATIONS
73	Automatic Speech Recognition Systems for the Evaluation of Voice and Speech Disorders in Head and Neck Cancer. Eurasip Journal on Audio, Speech, and Music Processing, 2010, 2010, 1-7.	1.3	33
74	Single-breath-hold 3-D CINE imaging of the left ventricle using Cartesian sampling. Magnetic Resonance Materials in Physics, Biology, and Medicine, 2018, 31, 19-31.	1.1	33
75	Towards intelligent robust detection of anatomical structures in incomplete volumetric data. Medical Image Analysis, 2018, 48, 203-213.	7.0	33
76	Automatic multiâ€organ segmentation in dualâ€energy CT (DECT) with dedicated 3D fully convolutional DECT networks. Medical Physics, 2020, 47, 552-562.	1.6	33
77	Threeâ€dimensional anisotropic adaptive filtering of projection data for noise reduction in cone beam CT. Medical Physics, 2011, 38, 5896-5909.	1.6	32
78	Fiducial markerâ€based correction for involuntary motion in weightâ€bearing Câ€arm CT scanning of knees. Part I. Numerical modelâ€based optimization. Medical Physics, 2013, 40, 091905.	1.6	32
79	Reconstruction of scalar and vectorial components in X-ray dark-field tomography. Proceedings of the National Academy of Sciences of the United States of America, 2014, 111, 12699-12704.	3.3	32
80	Augmented realityâ€based feedback for technicianâ€inâ€theâ€loop Câ€arm repositioning. Healthcare Technology Letters, 2018, 5, 143-147.	1.9	32
81	A large-scale dataset for mitotic figure assessment on whole slide images of canine cutaneous mast cell tumor. Scientific Data, 2019, 6, 274.	2.4	32
82	SPATIAL DISTRIBUTION OF CHORIOCAPILLARIS IMPAIRMENT IN EYES WITH CHOROIDAL NEOVASCULARIZATION SECONDARY TO AGE-RELATED MACULAR DEGENERATION. Retina, 2020, 40, 428-445.	1.0	32
83	A completely annotated whole slide image dataset of canine breast cancer to aid human breast cancer research. Scientific Data, 2020, 7, 417.	2.4	32
84	Fully Automated Data-Driven Respiratory Signal Extraction From SPECT Images Using Laplacian Eigenmaps. IEEE Transactions on Medical Imaging, 2016, 35, 2425-2435.	5.4	31
85	Development and validation of a classification and scoring system for the diagnosis of oral squamous cell carcinomas through confocal laser endomicroscopy. Journal of Translational Medicine, 2016, 14, 159.	1.8	31
86	A deep learning based pipeline for optical coherence tomography angiography. Journal of Biophotonics, 2019, 12, e201900008.	1.1	31
87	Computerized Calculation of Mitotic Count Distribution in Canine Cutaneous Mast Cell Tumor Sections: Mitotic Count Is Area Dependent. Veterinary Pathology, 2020, 57, 214-226.	0.8	31
88	Scale-Space Anisotropic Total Variation for Limited Angle Tomography. IEEE Transactions on Radiation and Plasma Medical Sciences, 2018, 2, 307-314.	2.7	29
89	Toward Bridging the Simulated-to-Real Gap: Benchmarking Super-Resolution on Real Data. IEEE Transactions on Pattern Analysis and Machine Intelligence, 2019, 42, 1-1.	9.7	29
90	Modern machine-learning can support diagnostic differentiation of central and peripheral acute vestibular disorders. Journal of Neurology, 2020, 267, 143-152.	1.8	29

#	Article	IF	CITATIONS
91	Fast onlineâ€customized (FOCUS) parallel transmission pulses: A combination of universal pulses and individual optimization. Magnetic Resonance in Medicine, 2021, 85, 3140-3153.	1.9	29
92	Probabilistic noninvasive prediction of wall properties of abdominal aortic aneurysms using Bayesian regression. Biomechanics and Modeling in Mechanobiology, 2017, 16, 45-61.	1.4	28
93	A Multi-task Framework for Skin Lesion Detection and Segmentation. Lecture Notes in Computer Science, 2018, , 285-293.	1.0	28
94	A Deep Learning Architecture for Limited-Angle Computed Tomography Reconstruction. Informatik Aktuell, 2017, , 92-97.	0.4	28
95	SlideRunner. Informatik Aktuell, 2018, , 309-314.	0.4	28
96	Fast simulation of x-ray projections of spline-based surfaces using an append buffer. Physics in Medicine and Biology, 2012, 57, 6193-6210.	1.6	27
97	A continuum description of the damage process in the arterial wall of abdominal aortic aneurysms. International Journal for Numerical Methods in Biomedical Engineering, 2012, 28, 87-99.	1.0	27
98	Electrophysiology Catheter Detection and Reconstruction From Two Views in Fluoroscopic Images. IEEE Transactions on Medical Imaging, 2016, 35, 567-579.	5.4	27
99	Photoluminescence for Defect Detection on Full-Sized Photovoltaic Modules. IEEE Journal of Photovoltaics, 2021, 11, 1419-1429.	1.5	27
100	Closing the Calibration Loop: An Inside-Out-Tracking Paradigm for Augmented Reality in Orthopedic Surgery. Lecture Notes in Computer Science, 2018, , 299-306.	1.0	27
101	The Central European Magdalenian. Vertebrate Paleobiology and Paleoanthropology, 2015, , .	0.1	26
102	Restoration of missing data in limited angle tomography based on Helgason–Ludwig consistency conditions. Biomedical Physics and Engineering Express, 2017, 3, 035015.	0.6	26
103	Quantifying the separability of data classes in neural networks. Neural Networks, 2021, 139, 278-293.	3.3	26
104	Correlation of biomechanics to tissue reaction in aortic aneurysms assessed by finite elements and [18F]–fluorodeoxyglucose–PET/CT. International Journal for Numerical Methods in Biomedical Engineering, 2012, 28, 456-471.	1.0	25
105	Fully automatic segmentation of left ventricular anatomy in 3-D LGE-MRI. Computerized Medical Imaging and Graphics, 2017, 59, 13-27.	3.5	25
106	GMM-Based Synthetic Samples for Classification of Hyperspectral Images With Limited Training Data. IEEE Geoscience and Remote Sensing Letters, 2018, 15, 942-946.	1.4	25
107	The Effect of Data Augmentation on Classification of Atrial Fibrillation in Short Single-Lead ECG Signals Using Deep Neural Networks. , 2020, , .		25
108	Synthetic Image Rendering Solves Annotation Problem in Deep Learning Nanoparticle Segmentation. Small Methods, 2021, 5, e2100223.	4.6	25

#	Article	IF	CITATIONS
109	Dynamic 2-D/3-D Rigid Registration Framework Using Point-To-Plane Correspondence Model. IEEE Transactions on Medical Imaging, 2017, 36, 1939-1954.	5.4	24
110	An in silico twin for epicardial augmentation of the failingÂheart. International Journal for Numerical Methods in Biomedical Engineering, 2019, 35, e3233.	1.0	24
111	Learning to detect anatomical landmarks of the pelvis in X-rays from arbitrary views. International Journal of Computer Assisted Radiology and Surgery, 2019, 14, 1463-1473.	1.7	24
112	A learningâ€based material decomposition pipeline for multiâ€energy xâ€ray imaging. Medical Physics, 2019, 46, 689-703.	1.6	24
113	Analysis and visualization of sleep stages based on deep neural networks. Neurobiology of Sleep and Circadian Rhythms, 2021, 10, 100064.	1.4	24
114	Improved reconstruction of phase-stepping data for Talbot–Lau x-ray imaging. Journal of Medical Imaging, 2017, 4, 1.	0.8	24
115	A Survey of Sensors in Healthcare Workflow Monitoring. ACM Computing Surveys, 2019, 51, 1-37.	16.1	23
116	Adapt Everywhere: Unsupervised Adaptation of Point-Clouds and Entropy Minimization for Multi-Modal Cardiac Image Segmentation. IEEE Transactions on Medical Imaging, 2021, 40, 1838-1851.	5.4	23
117	Interventional dualâ€energy imaging—Feasibility of rapid kVâ€switching on a Câ€arm CT system. Medical Physics, 2016, 43, 5537-5546.	1.6	22
118	Adaption of 3D Models to 2D X-Ray Images during Endovascular Abdominal Aneurysm Repair. Lecture Notes in Computer Science, 2015, , 339-346.	1.0	22
119	Spatial-temporal total variation regularization (STTVR) for 4D-CT reconstruction. Proceedings of SPIE, 2012, , .	0.8	21
120	Approaching prehistoric demography: proxies, scales and scope of the Cologne Protocol in European contexts. Philosophical Transactions of the Royal Society B: Biological Sciences, 2021, 376, 20190714.	1.8	21
121	Limited angle tomography for transmission X-ray microscopy using deep learning. Journal of Synchrotron Radiation, 2020, 27, 477-485.	1.0	21
122	Analysis of vertical and horizontal circular C-arm trajectories. Proceedings of SPIE, 2011, , .	0.8	20
123	Intraoperative stent segmentation in X-ray fluoroscopy for endovascular aortic repair. International Journal of Computer Assisted Radiology and Surgery, 2018, 13, 1221-1231.	1.7	20
124	ICDAR 2019 Competition on Image Retrieval for Historical Handwritten Documents. , 2019, , .		20
125	Analysis of continuous neuronal activity evoked by natural speech with computational corpus linguistics methods. Language, Cognition and Neuroscience, 2021, 36, 167-186.	0.7	20
126	Weakly Supervised Deep Learning-Based Optical Coherence Tomography Angiography. IEEE Transactions on Medical Imaging, 2021, 40, 688-698.	5.4	20

#	Article	IF	CITATIONS
127	Data Consistent Artifact Reduction for Limited Angle Tomography with Deep Learning Prior. Lecture Notes in Computer Science, 2019, , 101-112.	1.0	20
128	Automatic Speech Recognition Systems for the Evaluation of Voice and Speech Disorders in Head and Neck Cancer. Eurasip Journal on Audio, Speech, and Music Processing, 2010, 2010, 926951.	1.3	20
129	Implementation of machine learning into clinical breast MRI: Potential for objective and accurate decision-making in suspicious breast masses. PLoS ONE, 2020, 15, e0228446.	1.1	20
130	Automatically evaluated degree of intelligibility of children with different cleft type from preschool and elementary school measured by automatic speech recognition. International Journal of Pediatric Otorhinolaryngology, 2012, 76, 362-369.	0.4	19
131	Analyzing Relative Blood Flow Speeds in Choroidal Neovascularization Using Variable Interscan Time Analysis OCT Angiography. Ophthalmology Retina, 2018, 2, 306-319.	1.2	19
132	Fully Automated 3D Cardiac MRI Localisation and Segmentation Using Deep Neural Networks. Journal of Imaging, 2020, 6, 65.	1.7	19
133	A learning-based method for online adjustment of C-arm Cone-beam CT source trajectories for artifact avoidance. International Journal of Computer Assisted Radiology and Surgery, 2020, 15, 1787-1796.	1.7	19
134	EXACT: a collaboration toolset for algorithm-aided annotation of images with annotation version control. Scientific Reports, 2021, 11, 4343.	1.6	19
135	Auditory perceptible landmarks in mobile navigation. , 2007, , .		18
136	Automatic Quantification of Speech Intelligibility in Patients After Treatment for Oral Squamous Cell Carcinoma. Journal of Oral and Maxillofacial Surgery, 2011, 69, 1493-1500.	0.5	18
137	Approximate truncation robust computed tomography—ATRACT. Physics in Medicine and Biology, 2013, 58, 6133-6148.	1.6	18
138	Molecular RHD screening of RhD negative donors can replace standard serological testing for RhD negative donors. Transfusion and Apheresis Science, 2014, 50, 163-168.	0.5	18
139	Image artefact propagation in motion estimation and reconstruction in interventional cardiac C-arm CT. Physics in Medicine and Biology, 2014, 59, 3121-3138.	1.6	18
140	A Gauss-Seidel Iteration Scheme for Reference-Free 3-D Histological Image Reconstruction. IEEE Transactions on Medical Imaging, 2015, 34, 514-530.	5.4	18
141	Robust Multi-scale Anatomical Landmark Detection in Incomplete 3D-CT Data. Lecture Notes in Computer Science, 2017, , 194-202.	1.0	18
142	Precision Learning: Towards Use of Known Operators in Neural Networks. , 2018, , .		18
143	Browsing through sealed historical manuscripts by using 3-D computed tomography with low-brilliance X-ray sources. Scientific Reports, 2018, 8, 15335.	1.6	18
144	A Framework for Multiscale Quantitation of Relationships Between Choriocapillaris Flow Impairment and Geographic Atrophy Growth. American Journal of Ophthalmology, 2020, 214, 172-187.	1.7	18

#	Article	IF	CITATIONS
145	Will We Ever Have Conscious Machines?. Frontiers in Computational Neuroscience, 2020, 14, 556544.	1.2	18
146	Robust classification from noisy labels: Integrating additional knowledge for chest radiography abnormality assessment. Medical Image Analysis, 2021, 72, 102087.	7.0	18
147	Probe-based confocal laser endomicroscopy in detecting malignant lesions of vocal folds. Acta Otorhinolaryngologica Italica, 2019, 39, 389-395.	0.7	18
148	Computer-assisted mitotic count using a deep learning–based algorithm improves interobserver reproducibility and accuracy. Veterinary Pathology, 2022, 59, 211-226.	0.8	18
149	Consistencyâ€based respiratory motion estimation in rotational angiography. Medical Physics, 2017, 44, e113-e124.	1.6	17
150	Freeâ€breathing fat and R ₂ * quantification in the liver using a stackâ€ofâ€stars multiâ€echo acquisition with respiratoryâ€resolved modelâ€based reconstruction. Magnetic Resonance in Medicine, 2020, 84, 2592-2605.	1.9	17
151	Multi-task Localization and Segmentation for X-Ray Guided Planning in Knee Surgery. Lecture Notes in Computer Science, 2019, , 622-630.	1.0	17
152	Intrinsic Noise Improves Speech Recognition in a Computational Model of the Auditory Pathway. Frontiers in Neuroscience, 0, 16, .	1.4	17
153	Multi-Dimensional Flow-Preserving Compressed Sensing (MuFloCoS) for Time-Resolved Velocity-Encoded Phase Contrast MRI. IEEE Transactions on Medical Imaging, 2015, 34, 400-414.	5.4	16
154	Deformable respiratory motion correction for hepatic rotational angiography. Computerized Medical Imaging and Graphics, 2018, 66, 82-89.	3.5	16
155	NLO and off-shell effects in top quark mass determinations. Journal of High Energy Physics, 2018, 2018, 1.	1.6	16
156	Physicsâ€driven learning of xâ€ray skin dose distribution in interventional procedures. Medical Physics, 2019, 46, 4654-4665.	1.6	16
157	A combined experimental and theoretical study of radon solubility in fat and water. Scientific Reports, 2019, 9, 10768.	1.6	16
158	Multi-Modal Deep Guided Filtering for Comprehensible Medical Image Processing. IEEE Transactions on Medical Imaging, 2020, 39, 1703-1711.	5.4	16
159	Learning an Attention Model for Robust 2-D/3-D Registration Using Point-To-Plane Correspondences. IEEE Transactions on Medical Imaging, 2020, 39, 3159-3174.	5.4	16
160	A disease networkâ€based deep learning approach for characterizing melanoma. International Journal of Cancer, 2022, 150, 1029-1044.	2.3	16
161	Known operator learning and hybrid machine learning in medical imaging—a review of the past, the present, and the future. Progress in Biomedical Engineering, 2022, 4, 022002.	2.8	16
162	Bois Laiterie revisited: functional, morphological and technological analysis of a Late Glacial hunting camp in north-western Europe. Journal of Archaeological Science, 2011, 38, 1468-1484.	1.2	15

#	Article	IF	CITATIONS
163	Region-of-interest reconstruction on medical C-arms with the ATRACT algorithm. Proceedings of SPIE, 2012, , .	0.8	15
164	Comparison of Different Approaches for Measuring Tibial Cartilage Thickness. Journal of Integrative Bioinformatics, 2017, 14, .	1.0	15
165	Classification With Truncated <inline-formula> <tex-math notation="LaTeX">\$ell _{1}\$ </tex-math> </inline-formula> Distance Kernel. IEEE Transactions on Neural Networks and Learning Systems, 2018, 29, 2025-2030.	7.2	15
166	Dilated Convolutions in Neural Networks for Left Atrial Segmentation in 3D Gadolinium Enhanced-MRI. Lecture Notes in Computer Science, 2019, , 319-328.	1.0	15
167	Beyond the Alps and Tatra Mountains—the 20–14 ka Repopulation of the Northern Mid-latitudes as Inferred from Palimpsests Deciphered with Keys from Western and Central Europe. Journal of Paleolithic Archaeology, 2020, 3, 398-452.	0.7	15
168	Data Extrapolation From Learned Prior Images for Truncation Correction in Computed Tomography. IEEE Transactions on Medical Imaging, 2021, 40, 3042-3053.	5.4	15
169	DEDDIAG, a domestic electricity demand dataset of individual appliances in Germany. Scientific Data, 2021, 8, 176.	2.4	15
170	Age Determination of Children in Preschool and Primary School Age with GMM-Based Supervectors and Support Vector Machines/Regression. Lecture Notes in Computer Science, 2008, , 253-260.	1.0	15
171	Frangi-Net. Informatik Aktuell, 2018, , 341-346.	0.4	15
172	Recognizing Characters in Art History Using Deep Learning. , 2019, , .		15
173	Denoising and artefact reduction in dynamic flat detector CT perfusion imaging using high speed acquisition: first experimental and clinical results. Physics in Medicine and Biology, 2014, 59, 4505-4524.	1.6	14
174	A New Approach to the Evaluation of Forming Limits in Sheet Metal Forming. Key Engineering Materials, 2015, 639, 333-338.	0.4	14
175	<scp>MNS</scp> s genotyping by <scp>MALDI</scp> â€ <scp>TOF MS</scp> shows high concordance with serology, allows gene copy number testing and reveals new St(a) alleles. British Journal of Haematology, 2016, 174, 624-636.	1.2	14
176	Accurate laser scanner to camera calibration with application to range sensor evaluation. IPSJ Transactions on Computer Vision and Applications, 2017, 9, .	4.4	14
177	Higgs boson plus dijets: higher order corrections. Journal of High Energy Physics, 2017, 2017, 1.	1.6	14
178	Material Decomposition Using Ensemble Learning for Spectral X-ray Imaging. IEEE Transactions on Radiation and Plasma Medical Sciences, 2018, 2, 194-204.	2.7	14
179	Scanning trajectory optimisation using a quantitative Tuybased local quality estimation for robot-based X-ray computed tomography. Nondestructive Testing and Evaluation, 2020, 35, 287-303.	1.1	14
180	MR-contrast-aware image-to-image translations with generative adversarial networks. International Journal of Computer Assisted Radiology and Surgery, 2021, 16, 2069-2078.	1.7	14

#	Article	IF	CITATIONS
181	An Automated Deep Learning Method for Tile AO/OTA Pelvic Fracture Severity Grading from Trauma whole-Body CT. Journal of Digital Imaging, 2021, 34, 53-65.	1.6	14
182	Advanced neural networks for classification of MRI in psoriatic arthritis, seronegative, and seropositive rheumatoid arthritis. Rheumatology, 2022, 61, 4945-4951.	0.9	14
183	Evaluation of interpolation methods for surfaceâ€based motion compensated tomographic reconstruction for cardiac angiographic Câ€arm data. Medical Physics, 2013, 40, 031107.	1.6	13
184	Experimental setup for radon exposure and first diffusion studies using gamma spectroscopy. Nuclear Instruments & Methods in Physics Research B, 2015, 362, 187-193.	0.6	13
185	Kinect-Based Correction of Overexposure Artifacts in Knee Imaging with C-Arm CT Systems. International Journal of Biomedical Imaging, 2016, 2016, 1-15.	3.0	13
186	Highâ€resolution dynamic CEâ€MRA of the thorax enabled by iterative TWIST reconstruction. Magnetic Resonance in Medicine, 2017, 77, 833-840.	1.9	13
187	Unsupervised Learning for Robust Respiratory Signal Estimation From X-Ray Fluoroscopy. IEEE Transactions on Medical Imaging, 2017, 36, 865-877.	5.4	13
188	Higgs-boson plus dijets: higher-order matching for high-energy predictions. Journal of High Energy Physics, 2018, 2018, 1.	1.6	13
189	A comparison of methods for adapting 177Lu dose-voxel-kernels to tissue inhomogeneities. Physics in Medicine and Biology, 2019, 64, 245011.	1.6	13
190	Accurate fatty acid composition estimation of adipose tissue in the abdomen based on bipolar multiâ€echo MRI. Magnetic Resonance in Medicine, 2019, 81, 2330-2346.	1.9	13
191	Robust Multi-View 2-D/3-D Registration Using Point-To-Plane Correspondence Model. IEEE Transactions on Medical Imaging, 2020, 39, 161-174.	5.4	13
192	Task-Specific Trajectory Optimisation for Twin-Robotic X-Ray Tomography. IEEE Transactions on Computational Imaging, 2021, 7, 894-907.	2.6	13
193	X-ray Imaging. Lecture Notes in Computer Science, 2018, , 119-145.	1.0	13
194	OCT-OCTA segmentation: combining structural and blood flow information to segment Bruch's membrane. Biomedical Optics Express, 2021, 12, 84.	1.5	13
195	Anomaly detection in IR images of PV modules using supervised contrastive learning. Progress in Photovoltaics: Research and Applications, 2022, 30, 597-614.	4.4	13
196	Towards Clinical Application of a Laplace Operator-Based Region of Interest Reconstruction Algorithm in C-Arm CT. IEEE Transactions on Medical Imaging, 2014, 33, 593-606.	5.4	12
197	Scatter correction using a primary modulator on a clinical angiography Câ€arm CT system. Medical Physics, 2017, 44, e125-e137.	1.6	12
198	Range Imaging for Motion Compensation in C-Arm Cone-Beam CT of Knees under Weight-Bearing Conditions. Journal of Imaging, 2018, 4, 13.	1.7	12

#	Article	IF	CITATIONS
199	Temporal and volumetric denoising via quantile sparse image prior. Medical Image Analysis, 2018, 48, 131-146.	7.0	12
200	Determination of Forming Limits in Sheet Metal Forming Using Deep Learning. Materials, 2019, 12, 1051.	1.3	12
201	PMS-GAN: Parallel Multi-Stream Generative Adversarial Network for Multi-Material Decomposition in Spectral Computed Tomography. IEEE Transactions on Medical Imaging, 2021, 40, 571-584.	5.4	12
202	Intraoperative free margins assessment of oropharyngeal squamous cell carcinoma with confocal laser endomicroscopy: a pilot study. European Archives of Oto-Rhino-Laryngology, 2021, 278, 4433-4439.	0.8	12
203	Feasibility of intraoperative assessment of safe surgical margins during laryngectomy with confocal laser endomicroscopy: A pilot study. Auris Nasus Larynx, 2021, 48, 764-769.	0.5	12
204	JBFnet - Low Dose CT Denoising by Trainable Joint Bilateral Filtering. Lecture Notes in Computer Science, 2020, , 506-515.	1.0	12
205	Spatio-Temporal Handwriting Imitation. Lecture Notes in Computer Science, 2020, , 528-543.	1.0	12
206	Classification of Leukemic B-Lymphoblast Cells from Blood Smear Microscopic Images with an Attention-Based Deep Learning Method and Advanced Augmentation Techniques. Lecture Notes in Bioengineering, 2019, , 13-22.	0.3	12
207	Efficient and high accuracy 3-D OCT angiography motion correction in pathology. Biomedical Optics Express, 2021, 12, 125.	1.5	12
208	Deep Learning-Based Classification of Inflammatory Arthritis by Identification of Joint Shape Patterns—How Neural Networks Can Tell Us Where to "Deep Dive―Clinically. Frontiers in Medicine, 2022, 9, 850552.	1.2	12
209	Ultralowâ€parameter denoising: Trainable bilateral filter layers in computed tomography. Medical Physics, 2022, 49, 5107-5120.	1.6	12
210	Dynamic detector offsets for field of view extension in Câ€arm computed tomography with application to weightâ€bearing imaging. Medical Physics, 2015, 42, 2718-2729.	1.6	11
211	Real-Time Respiratory Motion Analysis Using 4-D Shape Priors. IEEE Transactions on Biomedical Engineering, 2016, 63, 485-495.	2.5	11
212	An Improved Extrapolation Scheme for Truncated CT Data Using 2D Fourier-Based Helgason-Ludwig Consistency Conditions. International Journal of Biomedical Imaging, 2017, 2017, 1-14.	3.0	11
213	Detecting Anatomical Landmarks for Motion Estimation in Weight-Bearing Imaging of Knees. Lecture Notes in Computer Science, 2018, , 83-90.	1.0	11
214	Co-localized augmented human and X-ray observers in collaborative surgical ecosystem. International Journal of Computer Assisted Radiology and Surgery, 2019, 14, 1553-1563.	1.7	11
215	Automated Billing Code Retrieval from MRI Scanner Log Data. Journal of Digital Imaging, 2019, 32, 1103-1111.	1.6	11
216	Finite quark-mass effects in Higgs boson production with dijets at large energies. Journal of High Energy Physics, 2019, 2019, 1.	1.6	11

#	Article	IF	CITATIONS
217	Robust Camera Pose Estimation for Unordered Road Scene Images in Varying Viewing Conditions. IEEE Transactions on Intelligent Vehicles, 2020, 5, 165-174.	9.4	11
218	Three-dimensional Monte Carlo-based voxel-wise tumor dosimetry in patients with neuroendocrine tumors who underwent 177Lu-DOTATOC therapy. Annals of Nuclear Medicine, 2020, 34, 244-253.	1.2	11
219	Deepâ€learningâ€based pipeline for module power prediction from electroluminescense measurements. Progress in Photovoltaics: Research and Applications, 2021, 29, 920-935.	4.4	11
220	Cephalogram synthesis and landmark detection in dental cone-beam CT systems. Medical Image Analysis, 2021, 70, 102028.	7.0	11
221	Monocular multi-person pose estimation: A survey. Pattern Recognition, 2021, 118, 108046.	5.1	11
222	Resolve Intraoperative Brain Shift as Imitation Game. Lecture Notes in Computer Science, 2018, , 129-137.	1.0	11
223	A Divide-and-Conquer Approach Towards Understanding Deep Networks. Lecture Notes in Computer Science, 2019, , 183-191.	1.0	11
224	Coronary Artery Plaque Characterization from CCTA Scans Using Deep Learning and Radiomics. Lecture Notes in Computer Science, 2019, , 593-601.	1.0	11
225	Dataset of Pages from Early Printed Books with Multiple Font Groups. , 2019, , .		11
226	Respiratory Motion Compensation Using Diaphragm Tracking for Cone-Beam C-Arm CT: A Simulation and a Phantom Study. International Journal of Biomedical Imaging, 2013, 2013, 1-10.	3.0	10
227	Patientâ€bounded extrapolation using lowâ€dose priors for volumeâ€ofâ€interest imaging in Câ€arm CT. Medical Physics, 2015, 42, 1787-1796.	1.6	10
228	Axially Extended-Volume C-Arm CT Using a Reverse Helical Trajectory in the Interventional Room. IEEE Transactions on Medical Imaging, 2015, 34, 203-215.	5.4	10
229	Accelerating multi-echo water-fat MRI with a joint locally low-rank and spatial sparsity-promoting reconstruction. Magnetic Resonance Materials in Physics, Biology, and Medicine, 2017, 30, 189-202.	1.1	10
230	Intraoperative Brain Shift Compensation Using a Hybrid Mixture Model. Lecture Notes in Computer Science, 2018, , 116-124.	1.0	10
231	Analysis of Forming Limits in Sheet Metal Forming with Pattern Recognition Methods. Part 1: Characterization of Onset of Necking and Expert Evaluation. Materials, 2018, 11, 1495.	1.3	10
232	Fast and Efficient Limited Data Hyperspectral Remote Sensing Image Classification via GMM-Based Synthetic Samples. IEEE Journal of Selected Topics in Applied Earth Observations and Remote Sensing, 2019, 12, 2107-2120.	2.3	10
233	Metric-Driven Learning of Correspondence Weighting for 2-D/3-D Image Registration. Lecture Notes in Computer Science, 2019, , 140-152.	1.0	10
234	Towards accelerated quantitative sodium MRI at 7ÂT in the skeletal muscle: Comparison of anisotropic acquisition- and compressed sensing techniques. Magnetic Resonance Imaging, 2021, 75, 72-88.	1.0	10

#	Article	IF	CITATIONS
235	SmartPatch: Improving Handwritten Word Imitation with Patch Discriminators. Lecture Notes in Computer Science, 2021, , 268-283.	1.0	10
236	Deep action learning enables robust 3D segmentation of body organs in various CT and MRI images. Scientific Reports, 2021, 11, 3311.	1.6	10
237	Radon Adsorption in Charcoal. International Journal of Environmental Research and Public Health, 2021, 18, 4454.	1.2	10
238	Learning to Avoid Poor Images: Towards Task-aware C-arm Cone-beam CT Trajectories. Lecture Notes in Computer Science, 2019, , 11-19.	1.0	10
239	Unsupervised Unstained Cell Detection by SIFT Keypoint Clustering and Self-labeling Algorithm. Lecture Notes in Computer Science, 2014, 17, 377-384.	1.0	10
240	Intelligibility of Children with Cleft Lip and Palate: Evaluation by Speech Recognition Techniques. , 2006, , .		9
241	Active contours methods with respect to Vickers indentations. Machine Vision and Applications, 2013, 24, 1183-1196.	1.7	9
242	Automatic Histogram-Based Initialization of K-Means Clustering in CT. Informatik Aktuell, 2013, , 277-282.	0.4	9
243	A Novel Framework for Interactive Visualization and Analysis of Hyperspectral Image Data. Journal of Electrical and Computer Engineering, 2016, 2016, 1-17.	0.6	9
244	Symmetry, outliers, and geodesics in coronary artery centerline reconstruction from rotational angiography. Medical Physics, 2017, 44, 5672-5685.	1.6	9
245	Factors affecting accuracy of S values and determination of time-integrated activity in clinical Lu-177 dosimetry. Annals of Nuclear Medicine, 2019, 33, 521-531.	1.2	9
246	Measuring Surface Area of Skin Lesions with 2D and 3D Algorithms. International Journal of Biomedical Imaging, 2019, 2019, 1-9.	3.0	9
247	U-Net for SPECT Image Denoising. , 2019, , .		9
248	Accelerated quantification of tissue sodium concentration in skeletal muscle tissue: quantitative capability of dictionary learning compressed sensing. Magnetic Resonance Materials in Physics, Biology, and Medicine, 2020, 33, 495-505.	1.1	9
249	Deep learning methods allow fully automated segmentation of metacarpal bones to quantify volumetric bone mineral density. Scientific Reports, 2021, 11, 9697.	1.6	9
250	Spatio-Temporal Multi-Task Learning for Cardiac MRI Left Ventricle Quantification. IEEE Journal of Biomedical and Health Informatics, 2021, 25, 2698-2709.	3.9	9
251	Classification of Confocal Laser Endomicroscopic Images of the Oral Cavity to Distinguish Pathological from Healthy Tissue. Informatik Aktuell, 2015, , 479-485.	0.4	9

252 Parallel-shift tomosynthesis for orthopedic applications. , 2018, , .

9

#	Article	IF	CITATIONS
253	How to Get the Most Out of U-Net for Glacier Calving Front Segmentation. IEEE Journal of Selected Topics in Applied Earth Observations and Remote Sensing, 2022, 15, 1712-1723.	2.3	9
254	Efficient 2D filtering for cone-beam VOI reconstruction. , 2012, , .		8
255	Free-Breathing Whole-Heart Coronary MRA: Motion Compensation Integrated into 3D Cartesian Compressed Sensing Reconstruction. Lecture Notes in Computer Science, 2013, 16, 575-582.	1.0	8
256	Scaling calibration in region of interest reconstruction with the 1D and 2D ATRACT algorithm. International Journal of Computer Assisted Radiology and Surgery, 2014, 9, 345-356.	1.7	8
257	A fully-automatic locally adaptive thresholding algorithm for blood vessel segmentation in 3D digital subtraction angiography. , 2015, 2015, 2006-9.		8
258	Open-source 4D statistical shape model of the heart for x-ray projection imaging. , 2015, , .		8
259	Image-based compensation for involuntary motion in weight-bearing C-arm cone-beam CT scanning of knees. Proceedings of SPIE, 2015, , .	0.8	8
260	OCPAD â€" Occluded checkerboard pattern detector. , 2016, , .		8
261	Rewiring of neuronal networks during synaptic silencing. Scientific Reports, 2017, 7, 11724.	1.6	8
262	Method for measurement of radon diffusion and solubility in solid materials. Nuclear Instruments & Methods in Physics Research B, 2018, 416, 119-127.	0.6	8
263	An MR-Based Model for Cardio-Respiratory Motion Compensation of Overlays in X-Ray Fluoroscopy. IEEE Transactions on Medical Imaging, 2018, 37, 47-60.	5.4	8
264	Individualized Biventricular Epicardial Augmentation Technology in a Drug-Induced Porcine Failing Heart Model. ASAIO Journal, 2018, 64, 480-488.	0.9	8
265	Traditional machine learning for limited angle tomography. International Journal of Computer Assisted Radiology and Surgery, 2019, 14, 11-19.	1.7	8
266	Application of Corneal Optical Coherence Tomography Angiography for Assessment of Vessel Depth in Corneal Neovascularization. Cornea, 2020, 39, 598-604.	0.9	8
267	ICFHR 2020 Competition on Image Retrieval for Historical Handwritten Fragments. , 2020, , .		8
268	Baptizo: A sensor fusion based model for tracking the identity of human poses. Information Fusion, 2020, 62, 1-13.	11.7	8
269	Deep Iterative 2D/3D Registration. Lecture Notes in Computer Science, 2021, , 383-392.	1.0	8
270	Combined subleading high-energy logarithms and NLO accuracy for W production in association with multiple jets. Journal of High Energy Physics, 2021, 2021, 1.	1.6	8

#	Article	IF	CITATIONS
271	X-Ray Scatter Estimation Using Deep Splines. IEEE Transactions on Medical Imaging, 2021, 40, 2272-2283.	5.4	8
272	RinQ Fingerprinting: Recurrence-Informed Quantile Networks for Magnetic Resonance Fingerprinting. Lecture Notes in Computer Science, 2019, , 92-100.	1.0	8
273	Automatic Classification and Pathological Staging of Confocal Laser Endomicroscopic Images of the Vocal Cords. Informatik Aktuell, 2017, , 312-317.	0.4	8
274	DNN-based Speed-of-Sound Reconstruction for Automated Breast Ultrasound. , 2020, , .		8
275	QMOS - a Robust Visualization Method for Speaker Dependencies With Different Microphones. Journal of Pattern Recognition Research, 2009, 4, 32-51.	0.9	8
276	Magnetic Resonance Fingerprinting Reconstruction Using Recurrent Neural Networks. Studies in Health Technology and Informatics, 2019, 267, 126-133.	0.2	8
277	Automated Multi-sequence Cardiac MRI Segmentation Using Supervised Domain Adaptation. Lecture Notes in Computer Science, 2020, , 300-308.	1.0	8
278	Boosting of Prosodic and Pronunciation Features to Detect Mispronunciations of Non-Native Children. , 2007, , .		7
279	Reverse vertical transmission of hepatitis B virus (HBV) infection from a transfusion-infected newborn to her mother. Journal of Hepatology, 2012, 56, 734-737.	1.8	7
280	The Added Value of Volume-of-Interest C-Arm CT Imaging during Endovascular Treatment of Intracranial Aneurysms. American Journal of Neuroradiology, 2016, 37, 660-666.	1.2	7
281	Patient-individualized boundary conditions for CFD simulations using time-resolved 3D angiography. International Journal of Computer Assisted Radiology and Surgery, 2016, 11, 1061-1069.	1.7	7
282	GMM Supervectors for Limited Training Data in Hyperspectral Remote Sensing Image Classification. Lecture Notes in Computer Science, 2017, , 296-306.	1.0	7
283	Automated left ventricle segmentation in 2-D LGE-MRI. , 2017, , .		7
284	Myocardial Scar Segmentation in LGE-MRI using Fractal Analysis and Random Forest Classification. , 2018, , .		7
285	Analysis of Forming Limits in Sheet Metal Forming with Pattern Recognition Methods. Part 2: Unsupervised Methodology and Application. Materials, 2018, 11, 1892.	1.3	7
286	Transferability of Deep Learning Algorithms for Malignancy Detection in Confocal Laser Endomicroscopy Images from Different Anatomical Locations of the Upper Gastrointestinal Tract. Communications in Computer and Information Science, 2019, , 67-85.	0.4	7
287	Pitfalls in interventional X-ray organ dose assessment—combined experimental and computational phantom study: application to prostatic artery embolization. International Journal of Computer Assisted Radiology and Surgery, 2019, 14, 1859-1869.	1.7	7
288	Symmetry prior for epipolar consistency. International Journal of Computer Assisted Radiology and Surgery, 2019, 14, 1541-1551.	1.7	7

#	Article	IF	CITATIONS
289	A Semi-Automated Usability Evaluation Framework for Interactive Image Segmentation Systems. International Journal of Biomedical Imaging, 2019, 2019, 1-21.	3.0	7
290	Segmentation, Classification, and Visualization of Orca Calls Using Deep Learning. , 2019, , .		7
291	A machine learning pipeline for internal anatomical landmark embedding based on a patient surface model. International Journal of Computer Assisted Radiology and Surgery, 2019, 14, 53-61.	1.7	7
292	ICDAR 2021 Competition on Historical Document Classification. Lecture Notes in Computer Science, 2021, , 618-634.	1.0	7
293	Implications of Experiment Set-Ups for Residential Water End-Use Classification. Water (Switzerland), 2021, 13, 236.	1.2	7
294	Are Fast Labeling Methods Reliable? A Case Study of Computer-Aided Expert Annotations on Microscopy Slides. Lecture Notes in Computer Science, 2020, , 24-32.	1.0	7
295	Deep Learning-Based Denoising of Mammographic Images Using Physics-Driven Data Augmentation. Informatik Aktuell, 2020, , 94-100.	0.4	7
296	Discrete Estimation of Data Completeness for 3D Scan Trajectories with Detector Offset. Informatik Aktuell, 2015, , 47-52.	0.4	7
297	Robust partial Fourier reconstruction for diffusionâ€weighted imaging using a recurrent convolutional neural network. Magnetic Resonance in Medicine, 2022, 87, 2018-2033.	1.9	7
298	In-vivo dose determination in a human after radon exposure: proof of principle. Radiation and Environmental Biophysics, 2022, 61, 279-292.	0.6	7
299	A multi-sensor architecture combining human pose estimation and real-time location systems for workflow monitoring on hybrid operating suites. Future Generation Computer Systems, 2022, 135, 283-298.	4.9	7
300	Neural network based successor representations to form cognitive mapsÂof space and language. Scientific Reports, 2022, 12, .	1.6	7
301	An automatic version of a reading disorder test. ACM Transactions on Speech and Language Processing, 2011, 7, 1-15.	0.9	6
302	Efficient focus assessment for a computer vision-based Vickers hardness measurement system. Journal of Electronic Imaging, 2012, 21, 021114.	0.5	6
303	A Robust Probabilistic Model for Motion Layer Separation in X-ray Fluoroscopy. Lecture Notes in Computer Science, 2015, 24, 288-299.	1.0	6
304	3-D printing based production of head and neck masks for radiation therapy using CT volume data: A fully automatic framework. , 2016, , .		6
305	A User-Centered Model for Usable Security and Privacy. Lecture Notes in Computer Science, 2017, , 74-89.	1.0	6
306	Prior-Free Respiratory Motion Estimation in Rotational Angiography. IEEE Transactions on Medical Imaging, 2018, 37, 1999-2009.	5.4	6

#	Article	IF	CITATIONS
307	Towards contextâ€sensitive CT imaging — organâ€specific image formation for single (SECT) and dual energy computed tomography (DECT). Medical Physics, 2018, 45, 4541-4557.	1.6	6
308	A 3-D Projection Model for X-ray Dark-field Imaging. Scientific Reports, 2019, 9, 9216.	1.6	6
309	Highâ€speed slotâ€scanning radiography using smallâ€angle tomosynthesis: Investigation of spatial resolution. Medical Physics, 2019, 46, 5454-5466.	1.6	6
310	Simultaneous reconstruction of multiple stiff wires from a single X-ray projection for endovascular aortic repair. International Journal of Computer Assisted Radiology and Surgery, 2019, 14, 1891-1899.	1.7	6
311	On Providing Multi-Level Quality of Service for Operating Rooms of the Future. Sensors, 2019, 19, 2303.	2.1	6
312	Speech intelligibility in patients with oral cancer: An objective baseline evaluation of pretreatment function and impairment. Head and Neck, 2019, 41, 1063-1069.	0.9	6
313	Impact of the nonâ€negativity constraint in modelâ€based iterative reconstruction from CT data. Medical Physics, 2019, 46, e835-e854.	1.6	6
314	Toward analyzing mutual interference on infrared-enabled depth cameras. Computer Vision and Image Understanding, 2019, 178, 1-15.	3.0	6
315	Simulation study on X-ray phase contrast imaging with dual-phase gratings. International Journal of Computer Assisted Radiology and Surgery, 2019, 14, 3-10.	1.7	6
316	An Assessment of Radiation Doses From Radon Exposures Using a Mouse Model System. International Journal of Radiation Oncology Biology Physics, 2020, 108, 770-778.	0.4	6
317	Assisting Maritime Search and Rescue (SAR) Personnel with Al-Based Speech Recognition and Smart Direction Finding. Journal of Marine Science and Engineering, 2020, 8, 818.	1.2	6
318	Known Operator Learning Enables Constrained Projection Geometry Conversion: Parallel to Cone-Beam for Hybrid MR/X-Ray Imaging. IEEE Transactions on Medical Imaging, 2020, 39, 3488-3498.	5.4	6
319	Drivers controlling spatial and temporal variation of microbial properties and dissolved organic forms (DOC and DON) in fen soils with persistently low water tables. Global Ecology and Conservation, 2021, 27, e01605.	1.0	6
320	The Potential of OMICs Technologies for the Treatment of Immune-Mediated Inflammatory Diseases. International Journal of Molecular Sciences, 2021, 22, 7506.	1.8	6
321	Towards Arbitrary Noise Augmentation—Deep Learning for Sampling from Arbitrary Probability Distributions. Lecture Notes in Computer Science, 2018, , 129-137.	1.0	6
322	Deriving Neural Network Architectures Using Precision Learning: Parallel-to-Fan Beam Conversion. Lecture Notes in Computer Science, 2019, , 503-517.	1.0	6
323	Contour-Based Bone Axis Detection for X-Ray Guided Surgery on the Knee. Lecture Notes in Computer Science, 2020, , 671-680.	1.0	6
324	Signal Decomposition for X-ray Dark-Field Imaging. Lecture Notes in Computer Science, 2014, 17, 170-177.	1.0	6

#	Article	IF	CITATIONS
325	Estimate, Compensate, Iterate: Joint Motion Estimation and Compensation in 4-D Cardiac C-arm Computed Tomography. Lecture Notes in Computer Science, 2015, , 579-586.	1.0	6
326	Robust Spectral Denoising for Water-Fat Separation in Magnetic Resonance Imaging. Lecture Notes in Computer Science, 2015, , 667-674.	1.0	6
327	Analysis of Hypernasal Speech in Children withÂCleftÂLipÂandÂPalate. Lecture Notes in Computer Science, 2008, , 389-396.	1.0	6
328	Synthetic Fundus Fluorescein Angiography using Deep Neural Networks. Informatik Aktuell, 2018, , 234-238.	0.4	6
329	Motion Artifact Detection in Confocal Laser Endomicroscopy Images. Informatik Aktuell, 2018, , 328-333.	0.4	6
330	Epipolar Consistency in Fluoroscopy for Image-Based Tracking. , 2015, , .		6
331	Epipolar Consistency Conditions for Motion Correction in Weight-Bearing Imaging. Informatik Aktuell, 2017, , 209-214.	0.4	6
332	Measuring CT Reconstruction Quality with Deep Convolutional Neural Networks. Lecture Notes in Computer Science, 2019, , 113-124.	1.0	6
333	Deep Learning Algorithms for Coronary Artery Plaque Characterisation from CCTA Scans. Informatik Aktuell, 2020, , 193-198.	0.4	6
334	Monte Carlo Dose Simulation for In-Vivo X-Ray Nanoscopy. Informatik Aktuell, 2022, , 107-112.	0.4	6
335	Limited parameter denoising for lowâ€dose Xâ€ray computed tomography using deep reinforcement learning. Medical Physics, 2022, 49, 4540-4553.	1.6	6
336	Patientâ€specific radiation riskâ€based tube current modulation for diagnostic CT. Medical Physics, 2022, 49, 4391-4403.	1.6	6
337	The use of automatic speech recognition showing the influence of nasality on speech intelligibility. European Archives of Oto-Rhino-Laryngology, 2010, 267, 1719-1725.	0.8	5
338	Voice Handicap and Health-Related Quality of Life after Treatment for Small Laryngeal Carcinoma. Folia Phoniatrica Et Logopaedica, 2011, 63, 122-128.	0.5	5
339	Reconstruction from truncated projections in cone-beam CT using an efficient 1D filtering. Proceedings of SPIE, 2013, , .	0.8	5
340	A realistic digital phantom for perfusion C-arm CT based on MRI data. , 2013, , .		5
341	Interventional heart wall motion analysis with cardiac C-arm CT systems. Physics in Medicine and Biology, 2014, 59, 2265-2284.	1.6	5
342	Super-resolved retinal image mosaicing. , 2016, , .		5

342 Super-resolved retinal image mosaicing. , 2016, , .

#	Article	IF	CITATIONS
343	Cryo-Balloon Catheter Localization Based on a Support-Vector-Machine Approach. IEEE Transactions on Medical Imaging, 2016, 35, 1892-1902.	5.4	5
344	Exhaustive graph cut-based vasculature reconstruction. , 2016, , .		5
345	Confidence-aware Levenberg-Marquardt optimization for joint motion estimation and super-resolution. , 2016, , .		5
346	Spatio-temporally regularized 4-D cardiovascular C-arm CT reconstruction using a proximal algorithm. , 2017, , .		5
347	Noise reduction in low-dose ct using a 3D multiscale sparse denoising autoencoder. , 2017, , .		5
348	Geometric primitive refinement for structured light cameras. Machine Vision and Applications, 2018, 29, 313-327.	1.7	5
349	Multiple Device Segmentation for Fluoroscopic Imaging Using Multi-task Learning. Lecture Notes in Computer Science, 2018, , 19-27.	1.0	5
350	Improving the identification of hedonic quality in user requirements: a second controlled experiment. Requirements Engineering, 2018, 23, 401-424.	2.1	5
351	Viewpoint planning for quantitative coronary angiography. International Journal of Computer Assisted Radiology and Surgery, 2018, 13, 1159-1167.	1.7	5
352	Robust mixed one-bit compressive sensing. Signal Processing, 2019, 162, 161-168.	2.1	5
353	Virtual cleaning and unwrapping of non-invasively digitized soiled bamboo scrolls. Scientific Reports, 2019, 9, 2311.	1.6	5
354	Mapping Ensembles of Trees to Sparse, Interpretable Multilayer Perceptron Networks. SN Computer Science, 2020, 1, 1.	2.3	5
355	Truncation Correction for X-ray Phase-Contrast Region-of-Interest Tomography. IEEE Transactions on Computational Imaging, 2020, 6, 625-639.	2.6	5
356	Influence of Inter-Annotator Variability on Automatic Mitotic Figure Assessment. Informatik Aktuell, 2021, , 241-246.	0.4	5
357	The Last Glacial Maximum in Europe – State of the Art in Geoscience and Archaeology. Quaternary International, 2021, 581-582, 1-6.	0.7	5
358	Impact of intraepithelial capillary loops and atypical vessels in confocal laser endomicroscopy for the diagnosis of laryngeal and hypopharyngeal squamous cell carcinoma. European Archives of Oto-Rhino-Laryngology, 2022, 279, 2029-2037.	0.8	5
359	Enhanced Magnetic Resonance Image Synthesis with Contrast-Aware Generative Adversarial Networks. Journal of Imaging, 2021, 7, 133.	1.7	5
360	Re-Ranking for Writer Identification and Writer Retrieval. Lecture Notes in Computer Science, 2020, , 572-586.	1.0	5

4

#	Article	IF	CITATIONS
361	Automatic CAD-RADS Scoring Using Deep Learning. Lecture Notes in Computer Science, 2020, , 45-54.	1.0	5
362	Automatic Removal of Externally Attached Fiducial Markers in Cone Beam C-Arm CT. Informatik Aktuell, 2014, , 318-323.	0.4	5
363	Maximum Likelihood Estimation of Head Motion Using Epipolar Consistency. Informatik Aktuell, 2019, , 134-139.	0.4	5
364	Learning-Based Correspondence Estimation for 2-D/3-D Registration. Informatik Aktuell, 2020, , 222-228.	0.4	5
365	Over-Exposure Correction in CT Using Optimization-Based Multiple Cylinder Fitting. Informatik Aktuell, 2015, , 35-40.	0.4	5
366	Data Completeness Estimation for 3D C-Arm Scans with Rotated Detector to Enlarge the Lateral Field-of-View. Informatik Aktuell, 2016, , 164-169.	0.4	5
367	Towards In-Vivo X-Ray Nanoscopy. Informatik Aktuell, 2018, , 115-120.	0.4	5
368	Manifold Learning-based Data Sampling for Model Training. Informatik Aktuell, 2018, , 269-274.	0.4	5
369	Assessment of measurement deviations: length-extended x-ray imaging for orthopedic applications. , 2019, , .		5
370	Classification of Body Regions Based on MRI Log Files. Advances in Intelligent Systems and Computing, 2018, , 102-109.	0.5	5
371	Mammographic breast density classification using a deep neural network: assessment on the basis of inter-observer variability. , 2019, , .		5
372	Understanding Compositional Structures in Art Historical Images Using Pose and Gaze Priors. Lecture Notes in Computer Science, 2020, , 109-125.	1.0	5
373	Field of View Extension in Computed Tomography Using Deep Learning Prior. Informatik Aktuell, 2020, , 186-191.	0.4	5
374	Systematic interpretation of confocal laser endomicroscopy: larynx and pharynx confocal imaging score. Acta Otorhinolaryngologica Italica, 2022, 42, 26-33.	0.7	5
375	Learning-based occupational x-ray scatter estimation. Physics in Medicine and Biology, 2022, 67, 075001.	1.6	5
376	Measurement of angles in time-of-flight data for the automatic supervision of training exercises. , 2010, , .		4
377	Shading correction for grating-based differential phase contrast X-ray imaging. , 2014, , .		4

Analog non-linear transformation-based tone mapping for image enhancement in C-arm CT., 2016, , .

#	Article	IF	CITATIONS
379	3-D reconstruction of historical documents using an X-Ray C-Arm CT system. , 2016, , .		4
380	Tibial cartilage creep during weight bearing: in vivo 3D CT assessment. Osteoarthritis and Cartilage, 2016, 24, S104.	0.6	4
381	Fast and robust selection of highly-correlated features in regression problems. , 2017, , .		4
382	Registration of vascular structures using a hybrid mixture model. International Journal of Computer Assisted Radiology and Surgery, 2019, 14, 1507-1516.	1.7	4
383	Guest editorial of the IJCARS—BVM 2018 special issue. International Journal of Computer Assisted Radiology and Surgery, 2019, 14, 1-2.	1.7	4
384	Estimating the Fundamental Matrix Without Point Correspondences With Application to Transmission Imaging. , 2019, , .		4
385	Calibrationâ€free beam hardening reduction in xâ€ray CBCT using the epipolar consistency condition and physical constraints. Medical Physics, 2019, 46, e810-e822.	1.6	4
386	Projection-to-Projection Translation for Hybrid X-ray and Magnetic Resonance Imaging. Scientific Reports, 2019, 9, 18814.	1.6	4
387	Peptides in proteins. Journal of Peptide Science, 2020, 26, e3235.	0.8	4
388	Art2Contour: Salient Contour Detection in Artworks Using Generative Adversarial Networks. , 2020, ,		4
389	C-arm CT imaging with the extended line-ellipse-line trajectory: first implementation on a state-of-the-art robotic angiography system. Physics in Medicine and Biology, 2020, 65, 185016.	1.6	4
390	Appearance Learning for Image-Based Motion Estimation in Tomography. IEEE Transactions on Medical Imaging, 2020, 39, 3667-3678.	5.4	4
391	Enhancing collaborative road scene reconstruction with unsupervised domain alignment. Machine Vision and Applications, 2021, 32, 1.	1.7	4
392	Hardware Failure Prediction on Imbalanced Times Series Data. Journal of Digital Imaging, 2021, 34, 182-189.	1.6	4
393	Double Your Views – Exploiting Symmetry in Transmission Imaging. Lecture Notes in Computer Science, 2018, , 356-364.	1.0	4
394	Deep Learning Based Metal Inpainting in the Projection Domain: Initial Results. Lecture Notes in Computer Science, 2019, , 125-136.	1.0	4
395	Projection and Reconstruction-Based Noise Filtering Methods in Cone Beam CT. Informatik Aktuell, 2015, , 59-64.	0.4	4
396	Projection-Based Denoising Method for Photon-Counting Energy-Resolving Detectors. Informatik Aktuell, 2015, , 137-142.	0.4	4

#	Article	IF	CITATIONS
397	Band-Pass Filter Design by Segmentation in Frequency Domain for Detection of Epithelial Cells in Endomicroscope Images. Informatik Aktuell, 2015, , 413-418.	0.4	4
398	Image Quality Analysis of Limited Angle Tomography Using the Shift-Variant Data Loss Model. Informatik Aktuell, 2016, , 277-282.	0.4	4
399	Maximum a posteriori signal recovery for optical coherence tomography angiography image generation and denoising. Biomedical Optics Express, 2021, 12, 55.	1.5	4
400	Patch-based Carcinoma Detection on Confocal Laser Endomicroscopy Images - A Cross-site Robustness Assessment. , 2018, , .		4
401	On Mathews Correlation Coefficient and Improved Distance Map Loss for Automatic Glacier Calving Front Segmentation in SAR Imagery. IEEE Transactions on Geoscience and Remote Sensing, 2022, 60, 1-12.	2.7	4
402	Low-Rank and Sparse Matrix Decomposition for Compressed Sensing Reconstruction of Magnetic Resonance 4D Phase Contrast Blood Flow Imaging (LoSDeCoS 4D-PCI). Lecture Notes in Computer Science, 2013, 16, 558-565.	1.0	4
403	A Feasibility Study of Automatic Multi-Organ Segmentation Using Probabilistic Atlas. Informatik Aktuell, 2017, , 218-223.	0.4	4
404	Multi-Modal Super-Resolution with Deep Guided Filtering. Informatik Aktuell, 2019, , 110-115.	0.4	4
405	Deep Representation Learning for Orca Call Type Classification. Lecture Notes in Computer Science, 2019, , 274-286.	1.0	4
406	Local weather conditions determine DOC production and losses from agricultural fen soils affected by open-pit lignite mining. Catena, 2022, 211, 106012.	2.2	4
407	Few-shot Unsupervised Domain Adaptation for Multi-modal Cardiac Image Segmentation. Informatik Aktuell, 2022, , 20-25.	0.4	4
408	Pixelwise Distance Regression for Glacier Calving Front Detection and Segmentation. IEEE Transactions on Geoscience and Remote Sensing, 2022, 60, 1-10.	2.7	4
409	Validity of tissue homogeneity in confocal laser endomicroscopy on the diagnosis of laryngeal and hypopharyngeal squamous cell carcinoma. European Archives of Oto-Rhino-Laryngology, 2022, 279, 4147-4156.	0.8	4
410	Logarithmic corrections to the QCD component of same-sign <mml:math xmlns:mml="http://www.w3.org/1998/Math/MathML" display="inline"><mml:mi>W</mml:mi> -pair production for vector boson scattering studies. Physical Review D, 2021, 104, .</mml:math 	1.6	4
411	Inter-species cell detection - datasets on pulmonary hemosiderophages in equine, human and feline specimens. Scientific Data, 2022, 9, .	2.4	4
412	Towards a language-independent intelligibility assessment of children with cleft lip and palate. , 2009, , .		3
413	Using the low-pass monogenic signal framework for cell/background classification on multiple cell lines in bright-field microscope images. International Journal of Computer Assisted Radiology and Surgery, 2014, 9, 379-386.	1.7	3
414	Effective one step-iterative fiducial marker-based compensation for involuntary motion in weight-bearing C-arm cone-beam CT scanning of knees. Proceedings of SPIE, 2014, , .	0.8	3

#	Article	IF	CITATIONS
415	Binarization Driven Blind Deconvolution for Document Image Restoration. Lecture Notes in Computer Science, 2015, , 91-102.	1.0	3
416	Comparative Evaluation of Interactive Segmentation Approaches. Informatik Aktuell, 2016, , 68-73.	0.4	3
417	Talbotâ€Lau Xâ€ray phase contrast for tilingâ€based acquisitions without reference scanning. Medical Physics, 2017, 44, 1886-1898.	1.6	3
418	Browsing through Closed Books: Fully Automatic Book Page Extraction from a 3-D X-Ray CT Volume. , 2017, , .		3
419	Long-term Outcome of Speech Intelligibility in Maxillary Dental Rehabilitation with Full Dentures: A Prospective Study Using Automatic Speech Quantification. International Journal of Prosthodontics, 2017, 30, 419-425.	0.7	3
420	Comparative Analysis of Unsupervised Algorithms for Breast MRI Lesion Segmentation. Informatik Aktuell, 2018, , 257-262.	0.4	3
421	Non-destructive Digitization of Soiled Historical Chinese Bamboo Scrolls. , 2018, , .		3
422	XDose: toward online cross-validation of experimental and computational X-ray dose estimation. International Journal of Computer Assisted Radiology and Surgery, 2021, 16, 1-10.	1.7	3
423	Learning-based Patch-wise Metal Segmentation with Consistency Check. Informatik Aktuell, 2021, , 4-9.	0.4	3
424	Deep Learning Compatible Differentiable X-ray Projections for Inverse Rendering. Informatik Aktuell, 2021, , 290-295.	0.4	3
425	Data-Driven Speed-of-Sound Reconstruction for Medical Ultrasound: Impacts of Training Data Format and Imperfections on Convergence. Lecture Notes in Computer Science, 2021, , 140-150.	1.0	3
426	Automatic Path Planning for Safe Guide Pin Insertion in PCL Reconstruction Surgery. Lecture Notes in Computer Science, 2021, , 560-570.	1.0	3
427	Self-Supervised Learning of Domain-Invariant Local Features for Robust Visual Localization Under Challenging Conditions. IEEE Robotics and Automation Letters, 2021, 6, 2753-2760.	3.3	3
428	Validation of a classification and scoring system for the diagnosis of laryngeal and pharyngeal squamous cell carcinomas by confocal laser endomicroscopy. Brazilian Journal of Otorhinolaryngology, 2022, 88, S26-S32.	0.4	3
429	ChainLineNet: Deep-Learning-Based Segmentation and Parameterization of Chain Lines in Historical Prints. Journal of Imaging, 2021, 7, 120.	1.7	3
430	Cell Detection for Asthma on Partially Annotated Whole Slide Images. Informatik Aktuell, 2021, , 147-152.	0.4	3
431	Random Forest Based Left Ventricle Segmentation in LGE-MRI. Lecture Notes in Computer Science, 2017, , 152-160.	1.0	3
432	Influence of Reading Errors on the Text-Based Automatic Evaluation of Pathologic Voices. Lecture Notes in Computer Science, 2008, , 325-332.	1.0	3

#	Article	IF	CITATIONS
433	Image-Based Detection of MRI Hardware Failures. Informatik Aktuell, 2019, , 206-211.	0.4	3
434	Prediction of MRI Hardware Failures based on Image Features Using Time Series Classification. Informatik Aktuell, 2020, , 131-136.	0.4	3
435	Respiratory Motion Compensation for C-Arm CT Liver Imaging. Informatik Aktuell, 2015, , 221-226.	0.4	3
436	3D Tensor Reconstruction in X-Ray Dark-Field Tomography. Informatik Aktuell, 2015, , 492-497.	0.4	3
437	A Joint Probabilistic Model for Speckle Variance, Amplitude Decorrelation and Interframe Variance (IFV) Optical Coherence Tomography Angiography. Informatik Aktuell, 2018, , 98-102.	0.4	3
438	Organ-specific context-sensitive CT image reconstruction and display. , 2018, , .		3
439	Reduktion von Metallartefakten durch multipositionale Datenfusion in der industriellen Röntgen-Computertomographie. TM Technisches Messen, 2020, 87, 101-110.	0.3	3
440	A Unified Bayesian Approach to Multi-Frame Super-Resolution and Single-Image Upsampling in Multi-Sensor Imaging. , 2015, , .		3
441	Deep OCT Angiography Image Generation for Motion Artifact Suppression. Informatik Aktuell, 2020, , 248-253.	0.4	3
442	Intelligibility Is More Than a Single Word: Quantification of Speech Intelligibility by ASR and Prosody. , 2007, , 278-285.		3
443	Merging-ISP: Multi-exposure High Dynamic Range Image Signal Processing. Lecture Notes in Computer Science, 2021, , 328-342.	1.0	3
444	FlexParser—The adaptive log file parser for continuous results in a changing world. Journal of Software: Evolution and Process, 2022, 34, .	1.2	3
445	Tibia Cortical Bone Segmentation in Micro-CT and X-ray Microscopy Data Using a Single Neural Network. Informatik Aktuell, 2022, , 333-338.	0.4	3
446	Radon Improves Clinical Response in an Animal Model of Rheumatoid Arthritis Accompanied by Increased Numbers of Peripheral Blood B Cells and Interleukin-5 Concentration. Cells, 2022, 11, 689.	1.8	3
447	Multi-Stage Platform for (Semi-)Automatic Planning in Reconstructive Orthopedic Surgery. Journal of Imaging, 2022, 8, 108.	1.7	3
448	Truncation correction for VOI C-arm CT using scattered radiation. Proceedings of SPIE, 2013, , .	0.8	2
449	Ein multifunktionales und energetisch aktives Fassadenelement aus Beton. Bautechnik, 2014, 91, 167-174.	0.2	2

450 Dual-energy C-arm CT in the angiographic suite. , 2015, , .

#	Article	IF	CITATIONS
451	Contrast-Based 3D/2D Registration of the Left Atrium: Fast versus Consistent. International Journal of Biomedical Imaging, 2016, 2016, 1-15.	3.0	2
452	Over-exposure correction in knee cone-beam CT imaging with automatic exposure control using a partial low dose scan. , 2016, , .		2
453	Bridge to real data: Empirical multiple material calibration for learning-based material decomposition. , 2016, , .		2
454	Coping with real world data: Artifact reduction and denoising for motion ompensated cardiac Câ€arm CT. Medical Physics, 2016, 43, 883-893.	1.6	2
455	Vesselness for text detection in historical document images. , 2016, , .		2
456	The 19th International Conference on Medical Image Computing and Computer-Assisted Intervention (MICCAI 2016). Medical Image Analysis, 2017, 41, 1.	7.0	2
457	Multi-View Depth-Aware Rigid 2-D/3-D Registration. , 2017, , .		2
458	Automated Curved and Multiplanar Reformation for Screening of the Proximal Coronary Arteries in MR Angiography. Journal of Imaging, 2018, 4, 124.	1.7	2
459	Fast Sample Generation with Variational Bayesian for Limited Data Hyperspectral Image Classification. , 2018, , .		2
460	Phase-Sensitive Region-of-Interest Computed Tomography. Lecture Notes in Computer Science, 2018, , 137-144.	1.0	2
461	Feasibility of Motion Compensation using Inertial Measurement in C-arm CT. , 2018, , .		2
462	Automatic Orientation Estimation of Inertial Sensors in C-Arm CT Projections. Current Directions in Biomedical Engineering, 2019, 5, 195-198.	0.2	2
463	Particle filter de-noising of voxel-specific time-activity-curves in personalized 177Lu therapy. Zeitschrift Fur Medizinische Physik, 2020, 30, 116-134.	0.6	2
464	α-Irradiation setup for primary human cell cultures. International Journal of Radiation Biology, 2020, 96, 206-213.	1.0	2
465	Expression of Melatonin Receptor 1 in Rat Mesenteric Artery and Perivascular Adipose Tissue and Vasoactive Action of Melatonin. Cellular and Molecular Neurobiology, 2020, 41, 1589-1598.	1.7	2
466	Improving Generalization Capability of Multiorgan Segmentation Models Using Dual-Energy CT. IEEE Transactions on Radiation and Plasma Medical Sciences, 2022, 6, 79-86.	2.7	2
467	Learning the Update Operator for 2D/3D Image Registration. Informatik Aktuell, 2021, , 117-122.	0.4	2
468	Automatic Chain Line Segmentation in Historical Prints. Lecture Notes in Computer Science, 2021, , 657-665.	1.0	2

#	Article	IF	CITATIONS
469	"Keep it simple, scholar†an experimental analysis of few-parameter segmentation networks for retinal vessels in fundus imaging. International Journal of Computer Assisted Radiology and Surgery, 2021, 16, 967-978.	1.7	2
470	Deep Learning-Based ECG-Free Cardiac Navigation for Multi-Dimensional and Motion-Resolved Continuous Magnetic Resonance Imaging. IEEE Transactions on Medical Imaging, 2021, 40, 2105-2117.	5.4	2
471	RGB-D-based Human Detection and Segmentation for Mobile Robot Navigation in Industrial Environments. , 2021, , .		2
472	Fast and Robust Detection of Solar Modules in Electroluminescence Images. Lecture Notes in Computer Science, 2019, , 519-531.	1.0	2
473	Simultaneous Estimation of X-Ray Back-Scatter and Forward-Scatter Using Multi-task Learning. Lecture Notes in Computer Science, 2020, , 199-208.	1.0	2
474	Automatic Plane Adjustment of Orthopedic Intraoperative Flat Panel Detector CT-Volumes. Lecture Notes in Computer Science, 2020, , 486-495.	1.0	2
475	Inertial Measurements for Motion Compensation in Weight-Bearing Cone-Beam CT of the Knee. Lecture Notes in Computer Science, 2020, , 14-23.	1.0	2
476	Move Over There: One-Click Deformation Correction for Image Fusion During Endovascular Aortic Repair. Lecture Notes in Computer Science, 2020, , 713-723.	1.0	2
477	3D Tele-Medical Speech Therapy using Time-of-Flight Technology. IFMBE Proceedings, 2009, , 1500-1503.	0.2	2
478	Objective vs.ÂSubjective Evaluation of Speakers with and without Complete Dentures. Lecture Notes in Computer Science, 2009, , 170-177.	1.0	2
479	Convolution-Based Truncation Correction for C-Arm CT Using Scattered Radiation. Informatik Aktuell, 2013, , 338-343.	0.4	2
480	Augmented Mitotic Cell Count Using Field of Interest Proposal. Informatik Aktuell, 2019, , 321-326.	0.4	2
481	Fourier Consistency-Based Motion Estimation in Rotational Angiography. Informatik Aktuell, 2017, , 110-115.	0.4	2
482	Detecting and Measuring Surface Area of Skin Lesions. Informatik Aktuell, 2018, , 29-34.	0.4	2
483	Towards Full-body X-ray Images. Informatik Aktuell, 2018, , 86-91.	0.4	2
484	Theoretically-exact filtered-backprojection reconstruction from real data on the line-ellipse-line trajectory. , 2019, , .		2
485	The Impact of Unfocused Vickers Indentation Images on the Segmentation Performance. Lecture Notes in Computer Science, 2012, , 468-478.	1.0	2
486	Evaluation of Spectrum Mismatching Using Spectrum Binning for Statistical Polychromatic Reconstruction in CT. Informatik Aktuell, 2014, , 42-47.	0.4	2

#	Article	IF	CITATIONS
487	Motion Compensation Using Range Imaging in C-Arm Cone-Beam CT. Communications in Computer and Information Science, 2017, , 561-570.	0.4	2
488	Application of deep learning algorithms for Lithographic mask characterization. , 2018, , .		2
489	SHAMANN: Shared Memory Augmented Neural Networks. Lecture Notes in Computer Science, 2019, , 830-841.	1.0	2
490	Asymmetric information in the German intraday electricity market. Energy Economics, 2020, 89, 104785.	5.6	2
491	Rigid and Non-Rigid Motion Compensation in Weight-Bearing CBCT of the Knee Using Simulated Inertial Measurements. IEEE Transactions on Biomedical Engineering, 2022, 69, 1608-1619.	2.5	2
492	Fully-Automatic CT Data Preparation for Interventional X-Ray Skin Dose Simulation. Informatik Aktuell, 2020, , 125-130.	0.4	2
493	The Notary in the Haystack – Countering Class Imbalance in Document Processing with CNNs. Lecture Notes in Computer Science, 2020, , 246-261.	1.0	2
494	Automatic Evaluation of Pathologic Speech – from Research to Routine Clinical Use. , 2007, , 294-301.		2
495	An Extension to the Sammon Mapping for the Robust Visualization of Speaker Dependencies. Lecture Notes in Computer Science, 2008, , 381-388.	1.0	2
496	Deep learning-based extended field of view computed tomography image reconstruction: influence of network design on image estimation outside the scan field of view. Biomedical Physics and Engineering Express, 2022, 8, 025021.	0.6	2
497	Fiducial marker recovery and detection from severely truncated data in navigationâ€assisted spine surgery. Medical Physics, 2022, 49, 2914-2930.	1.6	2
498	DiffServ-based Service-specific VCM in DVB-S2. , 2007, , .		1
499	Prospective, Paired Crossover Comparison of the in vitro Quality of Red Blood Cells Collected by the Automate for Blood Collection Device or by a Conventional Method. Transfusion Medicine and Hemotherapy, 2009, 36, 289-292.	0.7	1
500	An automatic screening test for preschool children. , 2009, , .		1
501	Improvement of a speech recognizer for standardized medical assessment of children's speech by integration of prior knowledge. , 2010, , .		1
502	Human-centric analysis of driver inattention. , 2013, , .		1
503	Dose reduction achieved by dynamically collimating the redundant rays in fan-beam and cone-beam CT. , 2013, , .		1
504	Edge-preserving bilateral filtering for images containing dense objects in CT. , 2013, , .		1

#	Article	IF	CITATIONS
505	Influence of the phase effect on gradientâ€based and statisticsâ€based focus measures in bright field microscopy. Journal of Microscopy, 2014, 254, 65-74.	0.8	1
506	A practical statistical polychromatic image reconstruction for computed tomography using spectrum binning. , 2014, , .		1
507	Approximate path seeking for statistical iterative reconstruction. , 2015, , .		1
508	Properties of the ellipse-line-ellipse trajectory with asymmetrical variations. , 2016, , .		1
509	CoronARe: A Coronary Artery Reconstruction Challenge. Lecture Notes in Computer Science, 2017, , 96-104.	1.0	1
510	Improving the Identification of Hedonic Quality in User Requirements $\hat{a} \in \rakeppi A$ Controlled Experiment. , 2017, , .		1
511	Sheet metal forming limits as classification problem. , 2017, , .		1
512	Traditional Machine Learning Techniques for Streak Artifact Reduction in Limited Angle Tomography. Informatik Aktuell, 2018, , 222-227.	0.4	1
513	Learning from a Handful Volumes: MRI Resolution Enhancement with Volumetric Super-Resolution Forests. , 2018, , .		1
514	Single-breath-hold abdominal \$\${T}_{1}\$\$ T 1 Â mapping using 3D Cartesian Look-Locker with spatiotemporal sparsity constraints. Magnetic Resonance Materials in Physics, Biology, and Medicine, 2018, 31, 399-414.	1.1	1
515	Dual-Mode Training with Style Control and Quality Enhancement for Road Image Domain Adaptation. , 2020, , .		1
516	Temporal and Spatial Detection of the Onset of Local Necking and Assessment of its Growth Behavior. Materials, 2020, 13, 2427.	1.3	1
517	Learning the Inverse Weighted Radon Transform. Informatik Aktuell, 2021, , 49-54.	0.4	1
518	Latent Shape Constraint for Anatomical Landmark Detection on Spine Radiographs. Informatik Aktuell, 2021, , 350-355.	0.4	1
519	A phantom study on dose efficiency for orthopedic applications: Comparing slotâ€scanning radiography using ultraâ€smallâ€angle tomosynthesis to conventional radiography. Medical Physics, 2021, 48, 2170-2184.	1.6	1
520	ForestNet – Automatic Design of Sparse Multilayer Perceptron Network Architectures Using Ensembles of Randomized Trees. Lecture Notes in Computer Science, 2020, , 32-45.	1.0	1
521	Semi-Automatic Basket Catheter Reconstruction from Two X-Ray Views. Lecture Notes in Computer Science, 2015, , 379-389.	1.0	1
522	User Loss A Forced-Choice-Inspired Approach to Train Neural Networks Directly by User Interaction. Informatik Aktuell, 2019, , 92-97.	0.4	1

1

#	Article	IF	CITATIONS
523	3D-Reconstruction of Stiff Wires from a Single Monoplane X-Ray Image. Informatik Aktuell, 2019, , 172-177.	0.4	1
524	Effects of Tissue Material Properties on X-Ray Image, Scatter and Patient Dose A Monte Carlo Simulation. Informatik Aktuell, 2019, , 270-275.	0.4	1
525	Tenfold your Photons. Informatik Aktuell, 2020, , 113-118.	0.4	1
526	Prediction of MRI Hardware Failures Based on Image Features Using Ensemble Learning. Informatik Aktuell, 2020, , 137-142.	0.4	1
527	Deep Autofocus with Cone-Beam CT Consistency Constraint. Informatik Aktuell, 2020, , 169-174.	0.4	1
528	Make the Most of Time Temporal Extension of the iTV Algorithm for 4D Cardiac C-Arm CT. Informatik Aktuell, 2016, , 170-175.	0.4	1
529	A Kernel Ridge Regression Model for Respiratory Motion Estimation in Radiotherapy. Informatik Aktuell, 2017, , 155-160.	0.4	1
530	Myocardial Twist from X-ray Angiography. Informatik Aktuell, 2018, , 365-370.	0.4	1
531	Geometric modeling of the aortic inner and outer vessel wall from CTA for aortic dissection analysis. , 2018, , .		1
532	Exploring the space between smoothed and non-smooth total variation for 3D iterative CT reconstruction. , 2019, , .		1
533	Motion gradients for epipolar consistency. , 2019, , .		1
534	C-arm CT imaging using the extended line-ellipse-line trajectory: seamless FBP reconstruction from real data. , 2020, , .		1
535	Field of Interest Proposal for Augmented Mitotic Cell Count: Comparison of Two Convolutional Networks. , 2019, , .		1
536	Scaling Calibration in the ATRACT Algorithm. Informatik Aktuell, 2013, , 104-109.	0.4	1
537	Fast Interpolation of Dense Motion Fields from Synthetic Phantoms. Informatik Aktuell, 2014, , 168-173.	0.4	1
538	Respiratory Motion Estimation Using a 3D Diaphragm Model. Informatik Aktuell, 2014, , 240-245.	0.4	1
539	Distance error correction for time-of-flight cameras. , 2017, , .		1

540 A hybrid approach for virtual clinical trials for mammographic imaging. , 2018, , .

#	Article	IF	CITATIONS
541	Decoupling Respiratory and Angular Variation in Rotational X-ray Scans Using a Prior Bilinear Model. Lecture Notes in Computer Science, 2019, , 583-594.	1.0	1
542	Noise reduction method in low-dose CT data combining neural networks and an iterative reconstruction technique. , 2019, , .		1
543	Deep Recurrent Partial Fourier Reconstruction in Diffusion MRI. Lecture Notes in Computer Science, 2020, , 38-47.	1.0	1
544	Investigation of Feature-Based Nonrigid Image Registration Using Gaussian Process. Informatik Aktuell, 2020, , 156-162.	0.4	1
545	Correction propagation for user-assisted optical coherence tomography segmentation: general framework and application to Bruch's membrane segmentation. Biomedical Optics Express, 2020, 11, 2830.	1.5	1
546	IJCARS: BVM 2021 special issue. International Journal of Computer Assisted Radiology and Surgery, 2021, 16, 2067-2068.	1.7	1
547	Training Deep Learning Models for 2D Spine X-rays Using Synthetic Images and Annotations Created from 3D CT Volumes. Informatik Aktuell, 2022, , 63-68.	0.4	1
548	HEJ 2.1: High-energy resummation with vector bosons and next-to-leading logarithms. Computer Physics Communications, 2022, 278, 108404.	3.0	1
549	Automatic plane adjustment of orthopedic intraoperative flat panel detector CT-volumes. Journal of Medical Imaging, 2022, 9, 034001.	0.8	1
550	One-Shot Object Detection in Heterogeneous Artwork Datasets. , 2022, , .		1
551	Single material beam hardening correction via an analytical energy response model for diagnostic CT. Medical Physics, 0, , .	1.6	1
552	Automatic classification of reading disorders in a single word reading test. , 2009, , .		0
553	Star Formation in the Turbulent Interstellar Medium and Its Implications on Galaxy Evolution. , 2009, , 79-91.		0
554	Analysis of three-dimensional joint space of the tibiofemoral joint. , 2013, , .		0
555	Guided noise reduction with streak removal for high speed flat detector CT perfusion. , 2013, , .		0
556	Left ventricular heart phantom for wall motion analysis. , 2013, , .		0
557	Einfluss von Bauwerksverformungen auf Fassadenkonstruktionen aus Glas am Beispiel der ETA-Fabrik. Stahlbau, 2016, 85, 207-217.	0.2	0
558	Reduction of Metal Artifacts Using a New Segmentation Approach. Informatik Aktuell, 2016, , 92-97.	0.4	0

#	Article	IF	CITATIONS
559	Editorial for the Special Issue on MICCAI 2015. Medical Image Analysis, 2016, 34, 1-2.	7.0	О
560	Dynamic pixel binning allows spatial and angular resolution tradeoffs to improve image quality in X-ray C-arm CT. , 2016, , .		0
561	Object removal in gradient domain of cone-beam CT projections. , 2016, , .		Ο
562	Automatic Finger Joint Detection for Volumetric Hand Imaging. Informatik Aktuell, 2016, , 104-109.	0.4	0
563	Guest editorial of the IJCARS MICCAI 2016 special issue. International Journal of Computer Assisted Radiology and Surgery, 2017, 12, 1243-1244.	1.7	Ο
564	Rapid Interactive and Intuitive Segmentation of 3D Medical Images Using Radial Basis Function Interpolation. Journal of Imaging, 2017, 3, 56.	1.7	0
565	Fourier-based Reduction of Directed Streak Artifacts in Cone-Beam CT. Informatik Aktuell, 2018, , 127-132.	0.4	Ο
566	Hyper-Hue and EMAP on Hyperspectral Images for Supervised Layer Decomposition of Old Master Drawings. , 2018, , .		0
567	Image Reconstruction with Variational Networks: Application to Synchrotron Radiation Imaging. , 2018, , .		Ο
568	Left Ventricle Segmentation in LGE-MRI: Filter Based vs. Learning Based. , 2018, , .		0
569	IJCARS: BVM 2019 special issue. International Journal of Computer Assisted Radiology and Surgery, 2019, 14, 1823-1824.	1.7	Ο
570	Inhomogeneous distribution of radon in different types of tissue in the human body. BIO Web of Conferences, 2019, 14, 03001.	0.1	0
571	Local topology preservation for vascular centerline matching using a hybrid mixture model. , 2019, , .		Ο
572	On the Value of the Non-negativity Constraint in CT. , 2019, , .		0
573	Characterization of carbon/glass hybrid unidirectional thermoplastic composite. Materials Today: Proceedings, 2021, 34, 356-359.	0.9	Ο
574	Ultrasound Breast Lesion Detection using Extracted Attention Maps from a Weakly Supervised Convolutional Neural Network. Informatik Aktuell, 2021, , 282-287.	0.4	0
575	Dataset on Bi- and Multi-nucleated Tumor Cells in Canine Cutaneous Mast Cell Tumors. Informatik Aktuell, 2021, , 134-139.	0.4	0
576	2D Respiration Navigation Framework for 3D Continuous Cardiac Magnetic Resonance Imaging. Informatik Aktuell, 2021, , 158-163.	0.4	0

#	Article	IF	CITATIONS
577	On the present habitats and ecology of Vertigo pseudosubstriata Ložek, 1954 (Mollusca, Gastropoda,) Tj ETQq Quaternary Science, 2021, 36, 1090-1100.	1 1 0.784 1.1	314 rgBT / <mark>O</mark> 0
578	Module-Power Prediction from PL Measurements using Deep Learning. , 2021, , .		0
579	Joint Superresolution and Rectification for Solar Cell Inspection. IEEE Journal of Photovoltaics, 2021, 11, 1051-1058.	1.5	0
580	Failure and Risk Analysis Based on Maintenance Reports of Machines Components in Manufacturing Industry. Mechanisms and Machine Science, 2022, , 278-286.	0.3	0
581	Comparison of methods for sensitivity correction in Talbot–Lau computed tomography. International Journal of Computer Assisted Radiology and Surgery, 2021, 16, 2099-2106.	1.7	Ο
582	Acquisition Parameter-conditioned Magnetic Resonance Image-to-image Translation. Informatik Aktuell, 2021, , 199-204.	0.4	0
583	3D Non-Rigid Alignment of Low-Dose Scans Allows to Correct for Saturation in Lower Extremity Cone-Beam CT. IEEE Access, 2021, 9, 71821-71831.	2.6	Ο
584	WEEDING IN THE GARDEN OF FORKING PATHS – YET ANOTHER LOOK AT ALTERNATE POSSIBILITIES. Grazer Philosophische Studien, 2008, 76, 228-235.	0.6	0
585	Towards the Automatic Classification of Reading Disorders in Continuous Text Passages. Lecture Notes in Computer Science, 2009, , 282-290.	1.0	0
586	Accelerated Centre-of-Gravity Calculation for Massive Numbers of Image Patches. Lecture Notes in Computer Science, 2012, , 566-574.	1.0	0
587	Adjoint Based Calibration of Coupled Simulation Approaches of Patient-Specific Vascular Models. , 2012, , .		0
588	Investigation of Single Photon Emission Computed Tomography Acquired on Helical Trajectories. Informatik Aktuell, 2015, , 504-509.	0.4	0
589	Preliminary Study Investigating Brain Shift Compensation using 3D CBCT Cerebral Vascular Images. Informatik Aktuell, 2018, , 163-168.	0.4	0
590	Classification of Polyethylene Particles and the Local CD3+ Lymphocytosis in Histological Slices. Informatik Aktuell, 2018, , 228-233.	0.4	0
591	Towards a dual phase grating interferometer on clinical hardware. , 2018, , .		0
592	On the Characteristics of Helical 3D X-Ray Dark-Field Imaging. Informatik Aktuell, 2019, , 264-269.	0.4	0
593	Workflow Phase Detection in Fluoroscopic Images Using Convolutional Neural Networks. Informatik Aktuell, 2019, , 191-196.	0.4	0
594	Respiratory Deformation Estimation in X-Ray-Guided IMRT Using a Bilinear Model. Informatik Aktuell, 2019, , 315-320.	0.4	0

#	Article	IF	CITATIONS
595	Detection of Unseen Low-Contrast Signals Using Classic and Novel Model Observers. Informatik Aktuell, 2019, , 212-217.	0.4	Ο
596	Isocenter Determination from Projection Matrices of a C-Arm CBCT. Informatik Aktuell, 2019, , 276-281.	0.4	0
597	Smooth Ride: Low-Pass Filtering of Manual Segmentations Improves Consensus. Informatik Aktuell, 2019, , 86-91.	0.4	0
598	Semi-Automatic Cell Correspondence Analysis Using Iterative Point Cloud Registration. Informatik Aktuell, 2019, , 116-121.	0.4	0
599	Multidimensional noise reduction in C-arm cone-beam CT via 2D-based Landweber iteration and 3D-based deep neural networks. , 2019, , .		Ο
600	Projection image-to-image translation in hybrid x-ray/MR imaging. , 2019, , .		0
601	Left ventricle segmentation in LGE-MRI using multiclass learning. , 2019, , .		0
602	Multi-Channel Volumetric Neural Network for Knee Cartilage Segmentation in Cone-Beam CT. Informatik Aktuell, 2020, , 67-72.	0.4	0
603	Imitation Learning Network for Fundus Image Registration Using a Divide-And-Conquer Approach. Informatik Aktuell, 2020, , 301-306.	0.4	0
604	Combining 2-D and 3-D Weight-Bearing X-Ray Images. Informatik Aktuell, 2020, , 335-340.	0.4	0
605	Feature Loss After Denoising of SPECT Projection Data using a U-Net. , 2020, , .		0
606	Eine sanfte Einf $ ilde{A}$ 1/4 hrung ins Lernen tiefer neuronaler Netze. , 2022, , 679-696.		0
607	ORCA-PARTY: An Automatic Killer Whale Sound Type Separation Toolkit Using Deep Learning. , 2022, , .		0
608	High-energy logarithmic corrections to the QCD component of same-sign W-pair production. SciPost Physics Proceedings, 2022, , .	0.2	0